Melting Can Hinder Impact-Induced Adhesion

Mostafa Hassani-Gangaraj,[1] David Veysset,[2,3] Keith A. Nelson,[2,3] and Christopher A. Schuh[1,*]
[1]*Department of Materials Science and Engineering, MIT, Cambridge, Massachusetts 02139, USA*
[2]*Institute for Soldier Nanotechnologies, MIT, Cambridge, Massachusetts 02139, USA*
[3]*Department of Chemistry, MIT, Cambridge, Massachusetts 02139, USA*
(Received 3 May 2017; published 25 October 2017)

Melting has long been used to join metallic materials, from welding to selective laser melting in additive manufacturing. In the same school of thought, localized melting has been generally perceived as an advantage, if not the main mechanism, for the adhesion of metallic microparticles to substrates during a supersonic impact. Here, we conduct the first *in situ* supersonic impact observations of individual metallic microparticles aimed at the explicit study of melting effects. Counterintuitively, we find that under at least some conditions melting is disadvantageous and hinders impact-induced adhesion. In the parameter space explored, i.e., ~ 10 μm particle size and ~ 1 km/s particle velocity, we argue that the solidification time is much longer than the residence time of the particle on the substrate, so that resolidification cannot be a significant factor in adhesion.

DOI: 10.1103/PhysRevLett.119.175701

Understanding materials physics under impact has motivated extensive research in areas ranging from asteroid strikes [1] and ballistic deposition [2] to mechanochemical synthesis [3], materials failures [4,5], structural modification [6], and phase transformation [7]. Less conventionally, three decades ago, metallic powder particles were first observed to bond to metallic substrates under supersonic-impact conditions at low temperatures [8]. The notion of impact-induced adhesion, thereafter, has been implemented in powder processing through kinetic deposition or cold spray [9,10]. Kinetic deposition has proven successful in making coatings [11–13], in reclaiming damaged metallic surfaces [14], and in additively manufacturing bulk metallic materials [15].

In this area of impact science, researchers have repeatedly observed a material-dependent critical velocity [16,17], a threshold above which supersonic particles change their mode of interaction with the substrate from rebound to adhesion. A variety of proposals including adiabatic shear instability [16], oxide layer breakup [18], diffusion [19] and localized melting [20] have been put forth to explain the underlying mechanism(s) of impact-induced adhesion, each of which enjoys partial support from observational data. For instance, sharp jumps observed in the temperature and strain in Lagrangian impact simulations have been used to support an argument for adiabatic shear localization [16,21]. Experimental measurements of reduced oxide content in cold spray coatings as compared to initial powder feedstock underpins an argument for oxide layer breakup [22]. Small spherical ejecta found in the coating [20] or intermetallic detected at the interface [23] suggest localized melting or interdiffusion.

More consensus, however, has been attained around postmortem observations of material jets around the periphery of adhered particles [16,24,25]. We have recently, for the first time, conducted *in situ* observations of the impact behavior of individual supersonic metallic microparticles below and above the critical velocity and found that material ejection and jetting are crucial for adhesion [26,27]. We argued that neither shear localization nor melting are needed to account for material ejection. Rather, it can arise from the interaction of the impact-induced pressure wave with the contact periphery of the particle. As a result, we found that the critical adhesion velocity is directly related to the bulk speed of sound [26]. In our view, the key feature is a fast-traveling pressure wave that drives material ejection and jetting when it interacts with the leading edge of an impacting particle just a few nanoseconds after the first contact. Subsequently, oxide layer breakup, shear localization, melting, and the resultant viscous flow might be, in fact, trailing consequences of extensive jetting.

Our focus on impact-induced adhesion being a pressure-driven phenomenon therefore generally suggests that a temperature rise—and by extension melting—need not adopt a critical importance in this context. The purpose of the present work is to take an additional significant step forward in this line of reasoning, by targeting the process of impact melting specifically to evaluate its role in adhesion. Our approach in conducting impact adhesion experiments differs from the more common use of spray nozzles, which includes many complex variables that we wish to eliminate from consideration. For example, in a typical experiment where the expansion of a hot carrier gas accelerates thousands of particles together, the complex heat transfer and particle interactions lead to a general lack of specific knowledge on the individual particles' velocity, size, and temperature at the point of impact.

Here, on the other hand, we use an in-house-designed microscale ballistic test platform to accelerate individual micrometer-size metallic particles with a well-defined size and well-controlled temperature, to have them impact a substrate, and to record the entire deformation, rebound, or adhesion process in real time. What is more, our approach allows us to make a one-to-one correspondence between our postmortem observations of the adhered particles or impact residue and the instant of impact. As shown schematically in Fig. 1(a), a laser excitation pulse is focused onto a launching pad assembly, on top of which metallic particles are sitting. Through the ablation of a gold layer and rapid expansion of an elastomeric polyurea film, single particles are launched toward a metallic substrate. We use a high-frame-rate camera and a synchronized quasi-cw laser imaging pulse to observe the particle approach and impact on the substrate in real time. More details regarding the launching pad assembly preparation, the optical setup, and the image analysis have been reported [28].

Figure 1(b) shows some exemplar *in situ* images that we captured for individual supersonic microparticle impacts. The top image series shows a 15-μm Al particle as it approaches a Zn substrate, impacts it at 950 m/s, and undergoes extensive plastic deformation evidenced by the flattening of the rebounding particle. The bottom image series, on the other hand, shows a 15-μm Al particle impacting an Al substrate with virtually the same velocity but adhering to the substrate. We have conducted many such experiments with a wide range of impact velocities for Al impact on Al, Zn impact on Zn, and Al impact on Zn. We measured the rebound and impact velocities for each impact and calculated the ratio between the two, known as the coefficient of restitution (COR). Figure 1(c) shows the COR as a function of impact velocity. The apparent linear decrease in the coefficient of restitution is followed by a sharp decline to zero, indicating particle adhesion, for Al and Zn particles impacting matched materials. This reveals the existence of the critical velocity for adhesion for these cases.

In contrast, for Al impacting on Zn, we have never observed a single Al particle adhering to Zn even at very high impact velocities, close to 1400 m/s. While the Al-on-Al and Zn-on-Zn data points deviate from linearity in a concave-downward fashion and fall to zero with many clear observations of adhesion, the Al-on-Zn data points deviate from linearity in a concave-upward fashion instead. They apparently plateau at a roughly constant nonzero COR value at the high-velocity range. Although these velocities are far beyond the critical adhesion velocity for both of the two constituent metals, there is apparently no critical adhesion velocity, at least over the studied range, for the mismatched Al/Zn pair. For a second, similar mismatched pair (Al impacting Sn; see Fig. SM1 in Supplemental Material [29]), we see the same effect.

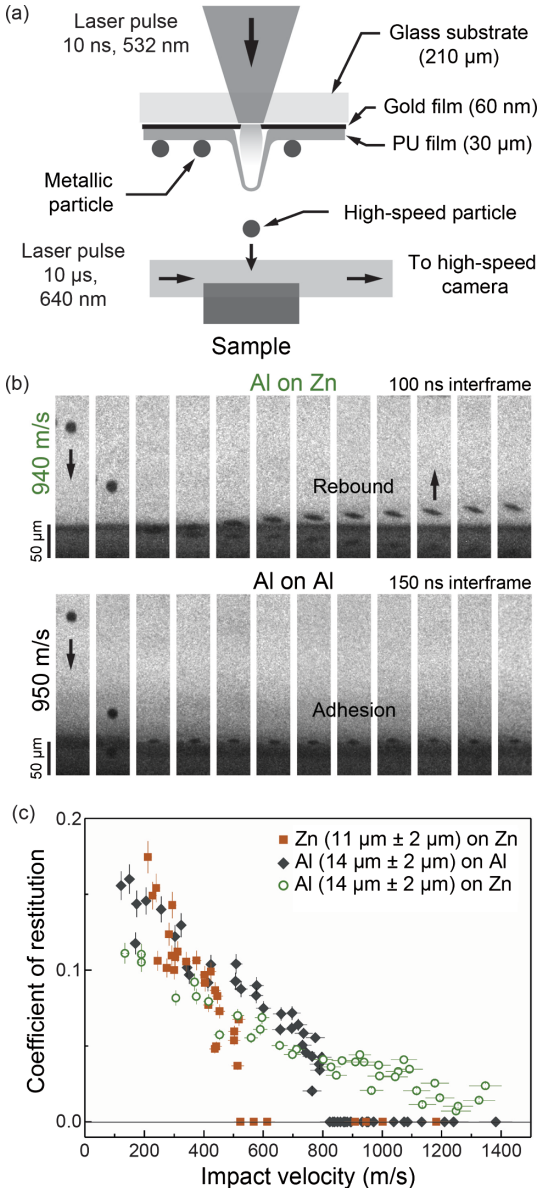

FIG. 1. *In situ* observation of a microparticle supersonic impact. (a) Experimental platform for the microparticle impact test and real-time imaging. (b) Multiframe sequences with 5 ns exposure times showing 15-μm Al particle impacts on a Zn substrate (top) and Al substrate (bottom) at 940 and 950 m/s, respectively, impact velocity. The microprojectile arrives from the top of the field of view. It rebounds after impacting on Zn but adheres to Al. (c) Coefficient of restitution for Al microparticle impacts on Al and Zn as well as Zn microparticle impacts on Zn. The coefficient of restitution is equal to zero above the critical velocity.

This is an anomalous finding and somewhat unexpected in light of the normal behavior of the Al-Al and Zn-Zn data. Site-specific observations of such impacts enable us to make a one-to-one correspondence between impact residue and the recorded impact event in the ~10 ns–10 μm–1 km/s time-size-velocity parameter space. The scanning electron microscope (SEM) images,

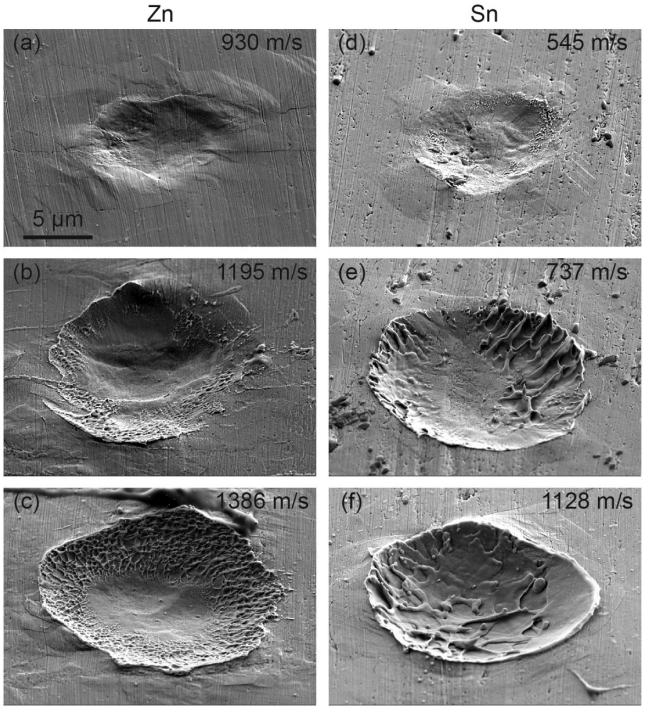

FIG. 2. SEM observation of Al microparticle supersonic impact-induced indentations on a Zn substrate at 930 (a), 1195 (b), and 1368 m/s (c) velocities along the impact-induced indentations on Sn at 545 (d), 737 (e), and 1128 m/s (f) velocities. Even though the substrate melted at increasing impact velocities, melting clearly did not lead to adhesion.

shown in the left column in Fig. 2, correspond to three impressions left behind after impacts of Al particles on Zn substrates at 930, 1195, and 1368 m/s. An impact at 930 m/s left an appreciable indentation behind. The surface morphology inside the indentation is similar to that of the undeformed substrate outside; the substrate has been deformed plastically but not melted and resolidified. With a further increase in the impact velocity, a ring with a netlike structure—a signature of melting and rupture through a Rayleigh-Taylor instability [32]—emerged close to the indentation edge. Energy dispersive spectroscopy (EDS) analysis (see Fig. SM2 in Supplemental Material [29]) of the impacted area confirmed that the netlike structure consists of the Zn substrate only, with no measurable contribution from the Al particle. In other words, it is the Zn substrate that undergoes melting and resolidification, and not the Al particle, in line with the fact that Zn has a lower melting temperature than Al (693 vs 933 K). The ring is only partial at the lower impact velocity but complete at the higher velocity. Interestingly, the impact velocity range causing melting is the same for which we observed the plateau of low but nonzero COR values in Fig. 1(c).

Based on these observations, we propose that the anomalous lack of adhesion in this case is caused by the emergence of melting, which hinders impact-induced adhesion. To further confirm this, we conducted the same experiments with the same Al microparticles but with a Sn substrate. Because of its lower specific heat and melting temperature, we expected Sn to be more susceptible to melting than Zn in our microparticle impact events. SEM images in the right column in Fig. 2 show three indentations on a Sn surface with increasing impact velocities. The same trend holds for this situation, albeit at much lower impact velocities for Sn than for Zn (by about 500 m/s) as expected. At 1128 m/s, the entire impact region underwent melting and resolidification; it is interesting that even a high-velocity impact producing such a large extent of melting could not lead to the adhesion of the impacting particle on the substrate.

While we cannot rule out a possible second change in behavior that admits adhesion at velocities above the range we are able to study here, the trends in the data suggest that more extensive melting does nothing to improve adhesion. This is in spite of the fact that melting should promote chemical interactions between the particle and substrate; whereas there is little solid solubility between these mismatched pairs, in the liquid Al-Zn is fully miscible and Al-Sn attains full miscibility if there is sufficient superheat in the liquid [33]. Similarly, the surface energy of Al is 1.16 J/m^2, and that of both Zn (0.99 J/m^2) and Sn (0.7 J/m^2) are much lower [34], which should correlate with a significant tendency to chemical mixing. Thus, as we increase the velocity to 1.4 times the threshold for melting in Al-Zn, we expect more chemical interaction that would favor bonding but see no hint of adhesion. In the case of Al-Sn, it is even more stark: Even at velocities up to 2.25 times the melting onset, we find no cases of adhesion.

These observations, far from supporting impact-induced melting as an adhesion mechanism, suggest the opposite; melting hinders adhesion in these experiments. Whereas melting fuses materials in welding [35] and bonds coatings to substrates during thermal spraying [36], it can oppose adhesion in a supersonic microparticle impact. We attribute this effect to the short time scales of supersonic adhesion. If an impacting particle resides on the top of a molten surface layer of a substrate for a long enough time, it should eventually fuse to the substrate thanks to chemical mixing and the molten layer resolidifying. In a supersonic impact, however, the residence time of the particle on the substrate is limited. If the time needed for solidification is longer than the residence time of the particle, it will rebound with no mechanical resistance from the adjacent unsolidified liquid.

For an order-of-magnitude-analysis, the residence time of the particle can be estimated with the characteristic time for a high-velocity impact:

$$t_r = \frac{d}{V_i} \tag{1}$$

with d being the diameter of the particle and V_i the impact velocity. The solidification time for a thin molten layer of

volume v_{melt} limited by heat conduction of the latent heat of fusion, H_f, out through an area A to the bulk of the substrate can be estimated using Chvorinov's rule [37]:

$$t_s = \left(\frac{H_f}{(T_m - T_0)}\right)^2 \left(\frac{\rho_s \pi}{4KC}\right) \left(\frac{v_{\mathrm{melt}}}{A}\right)^2, \tag{2}$$

where T_m is the melting temperature, T_0 is the ambient temperature, K is the thermal conductivity of the substrate, ρ_s is the density of the substrate, and C is the specific heat. In this analysis, for simplicity we neglect possible superheating and changes in properties of the substrate at melting.

We approximate the surface area of the melt with $A = \pi d^2/4$ and employ an energy scaling relationship to estimate the amount of molten material produced by a hypervelocity impact following [38]:

$$\frac{\rho_s v_{\mathrm{melt}}}{m_p} = k\left(\frac{V_i^2}{E_m}\right)^{3\mu/2}, \tag{3}$$

where m_p is the mass of the particle, k and μ are scaling parameters whose values have been constrained empirically [39,40], and E_m is the energy of the Rankine-Hugoniot state from which an adiabatic decompression would end on the liquidus at 1 atm (see Supplemental Material [29], which includes Refs. [30,31]).

In Fig. 3, we compare the solidification time for the melt induced by an impact of a 14-μm Al particle with the residence time of the particle at different impact velocities. We present the curves for Zn and Sn only for impact velocities beyond the corresponding threshold velocity of melting (~1000 and ~500 m/s, respectively) to keep the solidification time analysis relevant. At the threshold velocity for melting, the solidification time in both cases is at least 2 orders of magnitude higher than the residence time; the molten surface layer is unable to solidify (and thereby contribute to adhesion) during the time the particle is in contact with the substrate. At higher impact velocities, the residence time only decreases, while the solidification time rises, leading to very significant differences between the two parameters. At 1000 m/s, for instance, the solidification times for both Zn and Sn are in the microsecond regime, whereas the residence time remains in the nanosecond regime. Since the residence and solidification times are diverging at higher velocities in Fig. 3, this model suggests that it is unlikely that adhesion occurs at higher impact velocities beyond those explored in the present work.

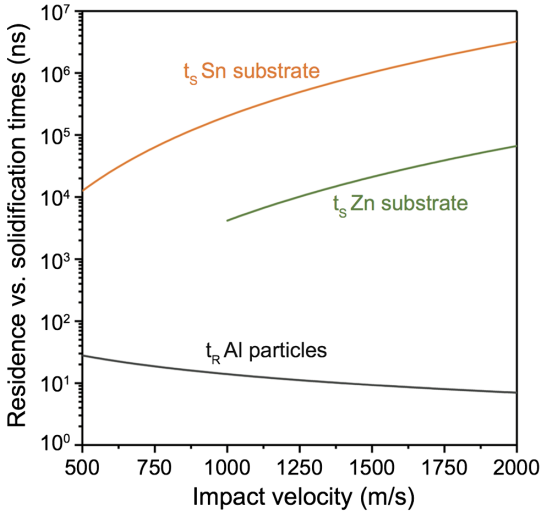

FIG. 3. Comparison of the residence time of a 14-μm Al particle with the solidification time of the impact-induced melt in Zn and Sn substrates. The solidification time for impact-induced melting by microparticles can be orders of magnitude longer than the residence time.

Setting the residence time equal to the solidification time leads to a potential domain where there could be a crossover between the two:

$$\left\{\frac{\pi k^2 \rho_p^2}{9KC\rho_s E_m^{3\mu}} \left(\frac{H_f}{T_m - T_0}\right)^2\right\} V_i^5 d = 1. \tag{4}$$

Equation (4) gives the locus of this crossover in the particle size-impact velocity space, with the amplitude in braces being a function of substrate properties and particle density ρ_p. We predict based on Eq. (4) that for much smaller (submicron) particles the residence time might be long enough to accommodate solidification while the particle is in contact, which might in turn facilitate adhesion ($t_R > t_S$) (see Fig. SM3 in Supplemental Material [29]). Although with our current platform it would be possible to launch submicron particles, such particle sizes are below the resolution of our imaging system, and we would not be capable of tracking them or measuring their velocities. We offer this as a direction for future work on this topic. Although the adhesion energy does not significantly differ from one metal to another, one may also study different materials for the particle and substrate to examine potential effects of the chemical nature between the two interacting materials.

In summary, our *in situ* and postmortem observations of a supersonic microparticle impact offer a contrary viewpoint to widely postulated benefits of localized melting in impact-induced adhesion: For ~10 μm particles, when an impact provides enough energy to melt the indent area, whether partially or fully, adhesion is found to be hindered; the low mechanical strength of the liquid interface is easily overcome by a rapidly rebounding particle if solidification is too slow to provide a solid-state joint. Such resolidification is estimated to take orders of magnitude longer than the time that the particle resides on the substrate. This mechanistic finding should prove useful for a broader understanding of impact-induced adhesion and particularly for the design of impact-based additive manufacturing processes.

This research was supported by the U.S. Army Research Office under Contract No. W911NF-13-D-0001. Support for equipment was also provided through the Office of Naval Research DURIP Grant No. N00014-13-1-0676.

*Corresponding author.
schuh@mit.edu

[1] J. E. Richardson, H. J. Melosh, and R. Greenberg, Science **306**, 1526 (2004).
[2] J. Blum and R. Schräpler, Phys. Rev. Lett. **93**, 115503 (2004).
[3] S. A. Humphry-Baker, S. Garroni, F. Delogu, and C. A. Schuh, Nat. Mater. **15**, 1280 (2016).
[4] T. Kadono and M. Arakawa, Phys. Rev. E **65**, 035107 (2002).
[5] A. Strachan, T. Cağin, and W. A. Goddard III, Phys. Rev. B **63**, 601031 (2001).
[6] S. M. Hassani-Gangaraj, K. S. Cho, H.-J. L. Voigt, M. Guagliano, and C. A. Schuh, Acta Mater. **97**, 105 (2015).
[7] P. S. Branicio, R. K. Kalia, A. Nakano, and P. Vashishta, Phys. Rev. Lett. **96**, 065502 (2006).
[8] A. Papyrin, V. Kosarev, S. Klinkov, A. Alkhimov, and V. M. Fomin, *Cold Spray Technology* (Elsevier Science, New York, 2006).
[9] H. Assadi, H. Kreye, F. Gärtner, and T. Klassen, Acta Mater. **116**, 382 (2016).
[10] A. Moridi, S. M. Hassani-Gangaraj, M. Guagliano, and M. Dao, Surf. Eng. **30**, 369 (2014).
[11] H. Koivuluoto, G. Bolelli, L. Lusvarghi, F. Casadei, and P. Vuoristo, Surf. Coat. Technol. **205**, 1103 (2010).
[12] E. Sansoucy, P. Marcoux, L. Ajdelsztajn, and B. Jodoin, Surf. Coat. Technol. **202**, 3988 (2008).
[13] A. Moridi, S. M. Hassani-Gangaraj, S. Vezzú, L. Trško, and M. Guagliano, Surf. Coat. Technol. **283**, 247 (2015).
[14] C. A. Widener, M. J. Carter, O. C. Ozdemir, R. H. Hrabe, B. Hoiland, T. E. Stamey, V. K. Champagne, and T. J. Eden, J. Therm. Spray Technol. **25**, 193 (2016).
[15] Y. Cormier, P. Dupuis, B. Jodoin, and A. Corbeil, J. Therm. Spray Technol. **25**, 170 (2016).
[16] H. Assadi, F. Gärtner, T. Stoltenhoff, and H. Kreye, Acta Mater. **51**, 4379 (2003).
[17] T. Schmidt, F. Gärtner, H. Assadi, and H. Kreye, Acta Mater. **54**, 729 (2006).
[18] W.-Y. Li, C.-J. Li, and H. Liao, Appl. Surf. Sci. **256**, 4953 (2010).
[19] S. Guetta, M. H. Berger, F. Borit, V. Guipont, M. Jeandin, M. Boustie, Y. Ichikawa, K. Sakaguchi, and K. Ogawa, J. Therm. Spray Technol. **18**, 331 (2009).
[20] G. Bae, S. Kumar, S. Yoon, K. Kang, H. Na, H.-J. Kim, and C. Lee, Acta Mater. **57**, 5654 (2009).
[21] M. Grujicic, C. L. Zhao, W. S. DeRosset, and D. Helfritch, Mater. Des. **25**, 681 (2004).
[22] W.-Y. Li, C. Zhang, H.-T. Wang, X. P. Guo, H. L. Liao, C.-J. Li, and C. Coddet, Appl. Surf. Sci. **253**, 3557 (2007).
[23] V. K. Champagne, M. K. West, M. Reza Rokni, T. Curtis, V. Champagne, and B. McNally, J. Therm. Spray Technol. **25**, 143 (2016).
[24] M. V. Vidaller, A. List, F. Gaertner, T. Klassen, S. Dosta, and J. M. Guilemany, J. Therm. Spray Technol. **24**, 644 (2015).
[25] P. C. King, C. Busch, T. Kittel-Sherri, M. Jahedi, and S. Gulizia, Surf. Coat. Technol. **239**, 191 (2014).
[26] M. Hassani-Gangaraj, D. Veysset, K. A. Nelson, and C. A. Schuh, arXiv:1612.08081.
[27] M. Hassani-Gangaraj, D. Veysset, K. A. Nelson, and C. A. Schuh, Scr. Mater. **145**, 9 (2018).
[28] D. Veysset, A. J. Hsieh, S. Kooi, A. A. Maznev, K. A. Masser, and K. A. Nelson, Sci. Rep. **6**, 25577 (2016).
[29] See Supplemental Material at http://link.aps.org/supplemental/10.1103/PhysRevLett.119.175701 for sample preparation, coefficient of restitutions for Al microparticle impacts on Sn, EDS analysis, and calculations of the energy term for melt volume analysis as well as solidification and residence time ratio maps for an Al particle impacting Zn and Sn. Supplemental Material includes Refs. [30,31].
[30] M. A. Meyers, *Dynamic Behavior of Materials* (Wiley, New York, 1994).
[31] M. B. Rubin and A. L. Yarin, Int. J. Impact Eng. **27**, 387 (2002).
[32] D. H. Sharp, Physica (Amsterdam) **12D**, 3 (1984).
[33] H. Okamoto, *Desk Handbook: Phase Diagrams for Binary Alloys* (American Society for Metals, Metals Park, OH, 2010).
[34] L. Vitos, A. V. Ruban, H. L. Skriver, and J. Kollár, Surf. Sci. **411**, 186 (1998).
[35] V. Avagyan, Phys. Rev. ST Accel. Beams **9**, 083501 (2006).
[36] H. Herman, S. Sampath, and R. McCune, MRS Bull. **25**, 17 (2000).
[37] J. Campbell, *Complete Casting Handbook: Metal Casting Processes, Metallurgy, Techniques and Design* (Elsevier Science, New York, 2015).
[38] M. D. Bjorkman and K. A. Holsapple, Int. J. Impact Eng. **5**, 155 (1987).
[39] E. Pierazzo, A. M. Vickery, and H. J. Melosh, Icarus **127**, 408 (1997).
[40] J. de Vries, F. Nimmo, H. J. Melosh, S. A. Jacobson, A. Morbidelli, and D. C. Rubie, Prog. Earth Planet. Sci. **3**, 7 (2016).